ACTA ABP BIOCHIMICA POLONICA

Vol. 59, No 1/2012
5–9
on-line at: www.actabp.pl

Review

Excited-state dynamics of overlapped optically-allowed $1B_u^+$ and optically-forbidden $1B_u^-$ or $3A_g^-$ vibronic levels of carotenoids: Possible roles in the light-harvesting function*

Yasushi Koyama[1]✉, Yoshinori Kakitani[1] and Hiroyoshi Nagae[2]

[1]Faculty of Science and Technology, Kwansei Gakuin University, Sanda, Japan; [2]Kobe City University of Foreign Studies, Gakuen Higashimachi, Kobe, Japan

Pump-probe spectroscopy after *selective excitation* of all-*trans* Cars (n = 9–13) in nonpolar solvent identified a symmetry selection rule of diabatic electronic mixing and diabatic internal conversion, i.e., '$1B_u^+$-to-$1B_u^-$ is allowed but $1B_u^+$-to-$3A_g^-$ is forbidden'. Kerr-gate fluorescence spectroscopy showed that this selection rule breaks down, due to the symmetry degradation when the Car molecules are being excited, and, as a result, the $1B_u^+$-to-$3A_g^-$ diabatic electronic mixing and internal conversion become allowed. On the other hand, pump-probe spectroscopy after *coherent excitation* of the same set of Cars in polar solvent identified three stimulated-emission components (generated by the quantum-beat mechanism), consisting of the long-lived coherent cross term from the $1B_u^+$ + $1B_u^-$ or $1B_u^+$ + $3A_g^-$ diabatic pair and incoherent short-lived $1B_u^+$ and $1B_u^-$ or $3A_g^-$ split incoherent terms. The same type of stimulated-emission components were identified in Cars bound to LH2 complexes, their lifetimes being substantially shortened by the Car-to-BChl singlet-energy transfer. Each diabatic pair and its split components appeared with high intensities in the first component. The low-energy shifts of the $1B_u^+(0)$, $1B_u^-(0)$ and $3A_g^-(0)$ levels and efficient triplet generation were also found.

Key words: carotenoids with 9–13 conjugated double bonds, optically-allowed ($1B_u^+$) and optically-forbidden ($1B_u^-$ or $3A_g^-$) states, overlapped (diabatic) states, incoherent/coherent excitation

Received: 17 October, 2011; accepted: 01 March, 2012;
available on-line: 17 March, 2012

1. INTRODUCTION

By Taven and Schulten (1987), linear relations of the optically-allowed $1B_u^+$ and the optically-forbidden $2A_g^-$, $1B_u^-$ and $3A_g^-$ singlet states were theoretically proposed. It was also shown that the slopes of the $2A_g^-$, $1B_u^-$ and $3A_g^-$ optically-forbidden singlet states, as functions of $1/(2n + 1)$, exhibit the ratio of ~2:3:4, respectively. The slopes of the $2A_g^-$, $1B_u^-$ and $3A_g^-$ states determined by measurement of resonance-Raman excitation profiles of crystalline Cars (n = 9–13) turned out to be 2:3.1:3.8 (Fig. 1a; Furuichi *et al.*, 2002), were in excellent agreement with those determined by a theoretical calculation, i.e., 2:3.1:3.7 (Tavan & Schulten, 1986).

Here, attention was focused on the overlap of $1B_u^+$-to-$1B_u^-$ and $1B_u^+$-to-$3A_g^-$ vibronic levels, shown in Fig. 1b. Then, experiments were designed to excite more than two different vibronic levels *coherently* (in phase) and to find out what kind of excited-state dynamics could be obtained.

In the Figure, we assumed sets of vibrational ladders with a spacing of ~1400 cm^{-1} (collectively considering the C=C and C–C stretchings and other vibrational modes). Then, the overlap of the vibrational ladders solely depended on the υ = 0 vibrational origins of the $1B_u^+$, $3A_g^-$, $1B_u^-$ and $2A_g^-$ singlet states shown in the linear relations in Fig. 1a. The energy gap of vibrational ladders in Car (n = 11) was the largest (300 cm^{-1}), whereas that in Car (n = 10) was practically negligible (0 cm^{-1}).

To change the conditions of excitation, two different pulse durations, i.e., 100 fs and 30 fs, were used. Figure 2 shows correlation between the pulse durations and the spectral widths. Here, the energy gap of 300 cm^{-1} in Car (n = 11) is an example. Then, the 100 fs pulse with a 200 cm^{-1} spectral width tends to *selectively* and *incoherently* excite the $1B_u^+(0)$ level, whereas the 30 fs pulse with a 700 cm^{-1} spectral width tends to *simultaneously* and *coherently* excites both the $1B_u^+(0)$ and $3A_g^-(1)$ levels. This is an extreme case but the situation can be more or less similar when the energy gap is smaller.

2. SELECTIVE, INCOHERENT EXCITATION BY 100 fs PULSES

(a) Pump-probe stimulated-emission spectroscopy: Excitation to the $1B_u^+(0)$ and $1B_u^+(1)$ levels of Cars (n = 9–13) in nonpolar solvents (Zuo *et al.*, 2007; Sutresno *et al.*, 2007)

Here, the Car molecules were excited to the $1B_u^+(0)$ and $1B_u^+(1)$ vibronic levels with 100 fs pulses with a high photon density from the A_g toward the B_u state. Then, the Pariser's ± signs lose their implication. (However, we will keep using the signs as formality.) Here, attention was focused on the patterns of the initial stimulated emission spectra. It turned out that *the stimulated emission* of the shorter-chain Cars (n = 9 and 10) consisted of two components, i.e., from the $1B_u^+$ and $1B_u^-$ vibronic levels, whereas *the stimulated emission* of the longer-chain

✉e-mail: ykoyama@kwansei.ac.jp

*Presented at the 16th International Symposium on Carotenoids, 17–22 July, 2011, Kraków, Poland

Abbreviations: Car(s), carotenoid(s); BChl(s), bacteriochlorophyll(s); 0 ← 0 excitation, excitation from the $1A_g^-(0)$ to the $1B_u^+(0)$ level; 1 ← 0 excitation, excitation from the $1A_g^-(0)$ to the $1B_u^+(1)$ level; n, number of conjugated double bonds; $1B_u^+(0)$, the υ = 0 vibrational level of the $1B_u^+$ electronic state; X-(υ), the $1B_u^-(1)$, $1B_u^-(2)$, $3A_g^-(1)$, $3A_g^-(2)$ and $3A_g^-(3)$ levels for Cars (n = 9, 10, 11, 12 and 13, respectively).

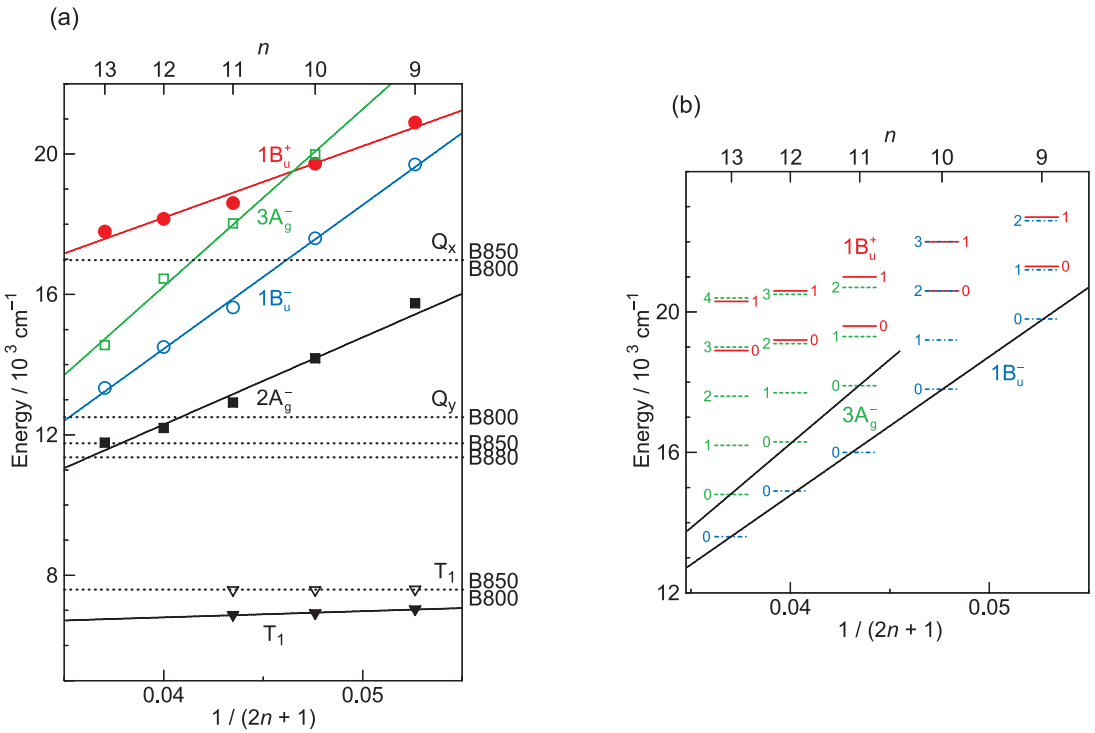

Figure 1. (a) Energies of the $1B_u^+(0)$, $3A_g^-(0)$, $1B_u^-(0)$ and $2A_g^-(0)$ vibronic levels of Cars (n = 9–13) free in solid and the T_1 state of Cars (n = 9–11) bound to LH2 complexes and the Q_x and Q_y levels of BChl *a* bound to LH2 (B800 and B850) and the LH1 (B880) complexes. (b) The vibrational ladder of the $1B_u^+$ state overlapped with those of the $1B_u^-$ states of Cars (n = 9 and 10) and the $3A_g^-$ states of Cars (n = 11–13).

Cars (n = 11–13), only one component, i.e., from the $1B_u^+$ vibronic level.

The results of simulation could be summarized as follows: *Shorter-chain Cars (n = 9 and 10):* After excitation to the $1B_u^+(0)$ level ('0 ← 0 excitation'), the observed stimulated emission could be explained in terms of *simultaneous stimulated emission* from the diabatic pairs, i.e., $1B_u^+(0)$ + $1B_u^-(1)$ and $1B_u^+(0)$ + $1B_u^-(2)$, respectively. After excitation to the $1B_u^+(1)$ level ('1 ← 0 excitation'), on the other hand, the vibrational relaxations of $1B_u^+(1)$ + $1B_u^-(2)$ → $1B_u^+(0)$ + $1B_u^-(1)$ and $1B_u^+(1)$ + $1B_u^-(3)$ → $1B_u^+(0)$ + $1B_u^-(2)$ took place, respectively, both accompanying the simultaneous stimulated emission.

Longer-chain Cars (n = 11–13): After 0 ← 0 excitation, only the $1B_u^+(0)$ stimulated emission was observed, whereas after the 1 ← 0 excitation, only the $1B_u^+(1)$ stimulated emission, instead. *Neither* the contribution of the $3A_g^-$ counterpart *nor* the vibrational relaxation in the $1B_u^+$ manifold was observed at all.

Thus, in both excitations, the direct $1B_u^+$ to $1B_u^-$ internal conversion took place, *skipping* the $3A_g^-$ state in-between. This is due to the absence of electronic mixing between the $1B_u^+$ + $3A_g^-$ diabatic pair and the presence of strong electronic interaction between the $1B_u^+$ and $1B_u^-$ vibronic pair. Thus, the reason why we did not see the $3A_g^-$ signal at all was explained. The above set of results lead us to a symmetry selection rule concerning the diabatic electronic mixing and internal conversion: '$1B_u^+$-to-$1B_u^-$ is allowed but $1B_u^+$-to-$3A_g^-$ is forbidden.'

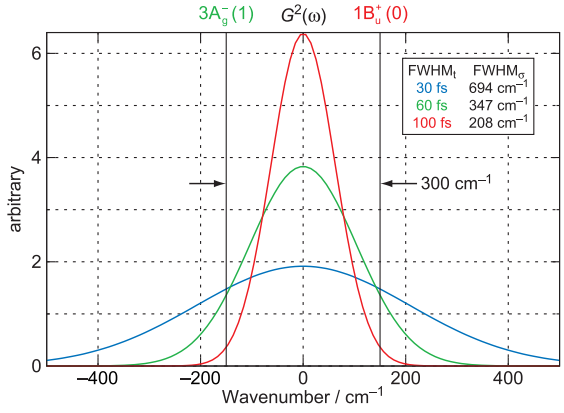

Figure 2. Correlation between pulse-duration and spectral-width.

(b) Kerr-gate fluorescence spectroscopy: Excitation to the $1B_u^+(3)$ or $1B_u^+(4)$ levels of Cars (n = 9–12) in nonpolar solvents (Kakitani *et al.*, 2009)

We tried to excite a set of Cars (n = 9–12) to the higher $1B_u^+$ vibronic levels to examine the effect of twisting of the conjugated chain upon excitation and the resultant breakdown of the above-mentioned symmetry selection rule due to symmetry degradation from C_{2h} to C_i.

(1) *In shorter-chain Cars (n = 9 and 10)*, the fluorescence patterns of components I and II (hereafter, abbreviated as 'fluorescence patterns I and II') consisted of fluorescence from the relevant $1B_u^+$ and $1B_u^-$ vibronic levels, although the fluorescence pattern II of Car (n = 10) contained fluorescence from the $3A_g^-$ vibronic levels, originating from the $3A_g^-$ state overlapped with the $1B_u^+$ state in the energy diagram (see Fig. 1a), and its splitting into two peaks was ascribable to a pair of molecules in the unit cell of an aggregate. Fluorescence pattern III was predominated by fluorescence from the $1B_u^+(0)$, because the $1B_u^-$ optically-forbidden component internally-converted to the isoenergetic $2A_g^-$ vibronic level.

(2) *In longer-chain Cars (n = 11 and 12)*, slightly-shaped, broad profiles of fluorescence patterns I, II and III could be simulated *partially* by fluorescence from the $1B_u^+(2)$, $1B_u^+(1)$ and $1B_u^+(0)$ vibronic levels but *predominantly* by a pair of fluorescence progressions from the $3A_g^-$ vibronic levels. The relative contributions of the above three fluorescence components exhibited no systematic changes at all.

Most importantly, we observed *not only* the $1B_u^+$-to-$1B_u^-$ diabatic electronic mixing in the shorter-chain Cars (n = 9 and 10) *but also* the $1B_u^+$-to-$3A_g^-$ diabatic electronic mixing in the longer-chain Cars (n = 11 and 12). The results indicated that symmetry degradation took place while the Car molecules were being vibronically excited, presumably due to the twisting of the conjugated chain around the C=C bonds. Then, the symmetry selection rule concerning the diabatic mixing broke down, and it became 'both the B_u-to-B_u and B_u-to-A_g mixing are allowed' (See, for the details, the reference listed in the title).

3. SIMULTANEOUS, COHERENT EXCITATION BY ~30 fs PULSES

The key results obtained here was the generation of quantum beat, consisting of the coherent cross term of the diabatic pair and the split incoherent terms of the diabatic counterparts. In the following subsections, descriptions will be made in the order, the split incoherent terms of the optically-forbidden counterparts and, then, the coherent cross term of the diabatic pair.

Here, we examine whether the excited-state dynamics of the same set of Cars free in solution (Fig. 3) are similar to, or different from, those bound to LH complexes (Fig. 4).

(a) Quantum beat in Cars (n = 9–11) in THF solution (Miki *et al.*, 2008; Li *et al.*, 2007)

In this and the next subsections, we are going to compare the excited-state dynamics between Cars free in solution and those bound to the LH2 complexes. This is the reason why we specifically choose Cars (n = 9–11). For simplicity, we will introduce, hereafter, a simplified expression, 'the $1B_u^+(0)$ + $X^-(\upsilon)$ diabatic pairs', where $X^-(\upsilon)$ indicates the $1B_u^-(1)$, $1B_u^-(2)$, $3A_g^-(1)$, $3A_g^-(2)$ and $3A_g^-(3)$ levels for Cars, n = 9, 10, 11, 12 and 13, respectively.

The time-resolved stimulated-emission and transient-absorption spectra (Fig. 3) can be characterized in terms of relaxation schemes shown in Fig. 5. This Figure explains a quantum-beat mechanism as follows: *Emission from the split counterparts.* Weak stimulated-emission peaks labeled $1B_u^-$ (blue) and $3A_g^-$ (green) have been found to have energies which fit the linear relations of the $1B_u^-$

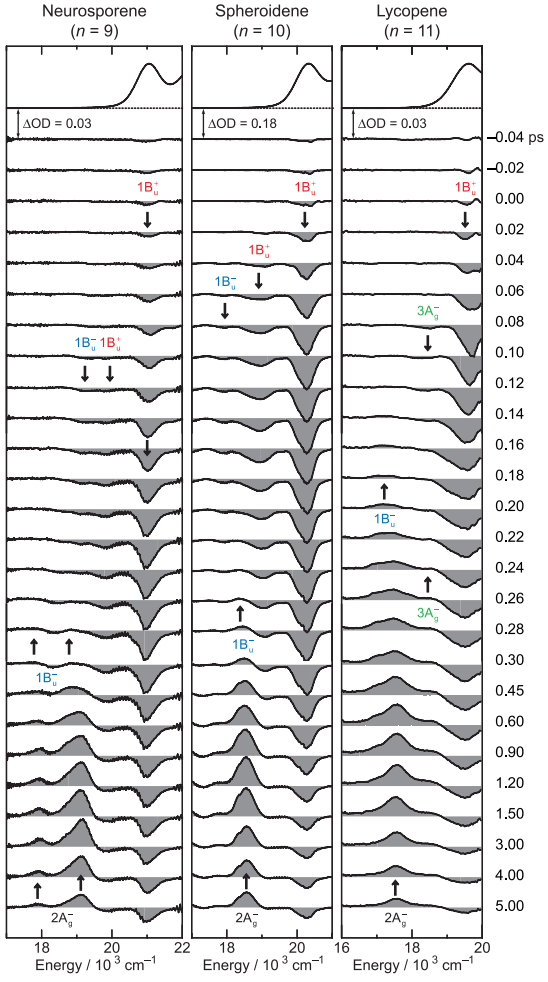

Figure 3. Time-resolved stimulated-emission and transient-absorption spectra after coherent excitation with 30 fs pulses, aiming at the $1B_u^+(0)$ level of Cars (n = 9–11) in THF solution.

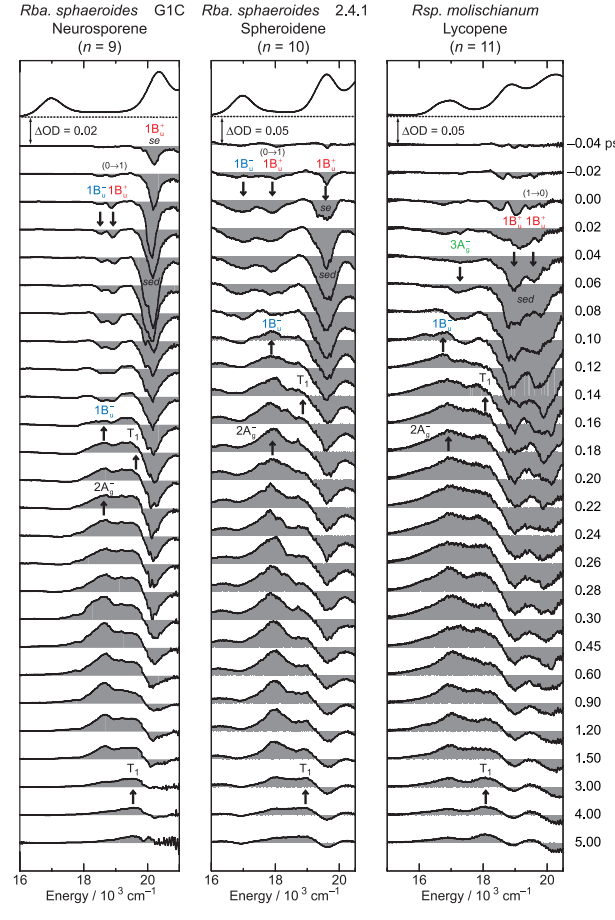

Figure 4. Time-resolved stimulated-emission and transient-absorption spectra after coherent excitation with 30 fs pulses, aiming at the $1B_u^+(0)$ level of Cars (n = 9–11) bound to LH2 antenna complexes.

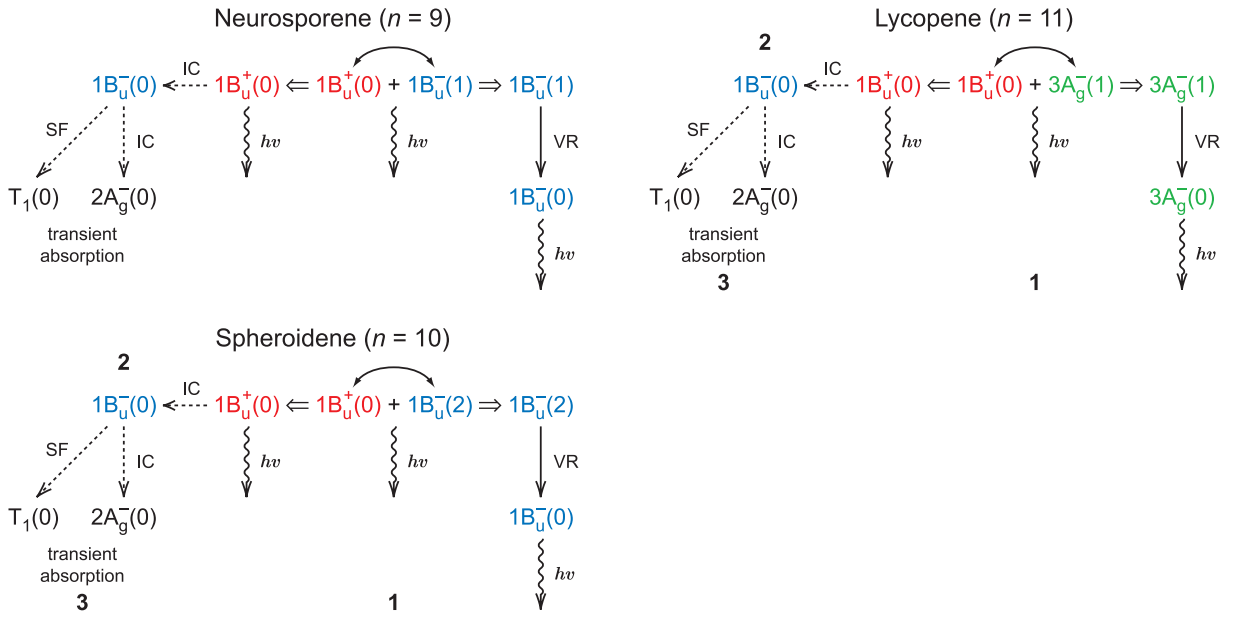

Figure 5. Relaxation schemes when Cars (n = 9–11) bound to LH2 complexes are coherently excited to the diabatic pairs.

(0) and $3A_g^-(0)$ levels as shown in Fig. 1a. Thus, they are ascribable to the results of splitting from the $1B_u^+(0)$ + $X^-(\upsilon)$ diabatic pair followed by vibrational relaxation. Weak emission peaks which are labeled '$1B_u^+$ (red)' can be ascribed to the transitions of the optically-allowed split counterpart, accompanying the optically-forbidden $1B_u^-$ (blue) or $3A_g^-$ (green) emission.

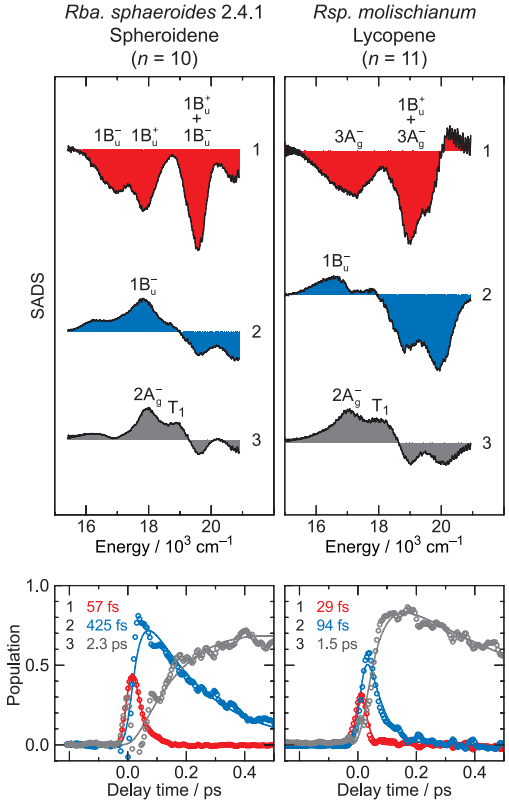

Figure 6. Comparison of SVD-global fitting analyses between Car (n = 10 and 11) bound to LH2 complexes from *Rba. sphaeroides* 2.4.1 and *Rsp. molischianum*: Species-associated difference spectra (SADS, upper panels) and time-dependent changes in population (lower panels).

Emission from the diabatic pair. Immediately after excitation ('0.02 ps' in Fig. 3), a weak peak appears at the (0 ← 0) peak position of the ground-state absorption (the top panels). This indicates that the $1B_u^+(0)$ counterpart is initially excited as a precursor. Subsequently, *much stronger and broader peaks* ascribable to the $1B_u^+(0)$ + $X^-(\upsilon)$ diabatic pairs grow and stay for a long time. Intuitively, back-and-forth transformation between the optically-allowed ($1B_u^+$) and optically-forbidden ($1B_u^-$ or $3A_g^-$) diabatic vibronic levels gives rise to such a long-lived emission peak (called 'persistent peak').

(b) Quantum beat and triplet generation in Cars (n = 9–11) bound to the LH2 complexes (Christiana *et al.*, 2009)

As shown in the previous subsection, the coherent excitation of Cars (n = 9–11) in a polar solvent exhibited *not only* the short-lived stimulated emission from the split and vibrationally-relaxed $1B_u^+(0)$ and $X^-(0)$ counterparts *but also* the strongly-coupled, long-lived emission from the $1B_u^+(0)$ + $X^-(\upsilon)$ diabatic pair, which had been explained in terms of the quantum-beat mechanism. Here, we examine whether the excited-state dynamics of the same set of Cars bound to the LH2 complexes are similar to, or different from, those free in solution.

The time-resolved stimulated-emission and transient-absorption spectra of the set of Cars bound to the LH2 complexes from *Rba. sphaeroides* G1C, *Rba. sphaeroides* 2.4.1 and *Rsp. molischianum* are presented in Fig. 4, which can be characterized as follows: *Emission from the split counterparts*. When bound to the LH2 complexes, basically the same set of the split counterparts, including $1B_u^+(0)$, $1B_u^-(0)$ and $3A_g^-(0)$, are seen but they appear almost immediately after excitation. It seems that the excited-state dynamics is strongly accelerated. Their energies were compared with those in THF solution (data not shown): All of the $1B_u^+(0)$, $1B_u^-(0)$ and $3A_g^-(0)$ levels were shifted downward in energy when compared with those in solution. Surprisingly, the shifts of the covalent $3A_g^-$ and $1B_u^-$ levels were larger than that of the ionic $1B_u^+$ level. This observation strongly suggests a strong polarization of the conjugated chain. *Emission from the diabatic pair*. When bound to the LH2 complexes, stimulated emis-

sion from the diabatic pair becomes much broader or even splits into two peaks, probably due to their strong coupling (Fig. 4). It becomes much stronger and more short-lived, indicating again the accelerated excited-state dynamics. *Transient absorptions.* Transient absorption from the T_1 state is clearly seen. Importantly, the branching of the $1B_u^-$ state into the $2A_g^-$ state and the T_1 state is suggested here spectroscopically, which is evidenced in Fig. 6.

The above characterization of the time-resolved spectra leads us to the overall relaxation scheme shown in Fig. 4. The observation of the $1B_u^+(0) + X^-(v)$ diabatic pair and the $1B_u^+(0)$ and $X^-(v)$ split counterparts evidences the quantum-beat mechanism. The appearance of the $1B_u^-$ transient absorption followed by the $2A_g^-$ and T_1 transient absorptions indicates the $1B_u^- \rightarrow 2A_g^-$ internal conversion plus the $1B_u^- \rightarrow T_1$ singlet fission branching processes. The latter process is most probably facilitated by the twisting of the conjugated chain due to the binding of the relevant Car to the apo-complex consisting of peptides and BChls.

Singular-value-decomposition (SVD) followed by global fitting of data matrices of a typical pair of Cars (n = 10 and n = 11), shown in Fig. 6, supports the above relaxation schemes: Timely, the relaxation takes place, in the order, (i) stimulated emission from the $1B_u^+(0) + 1B_u^-(2)$ or $1B_u^+(0) + 3A_g^-(1)$ diabatic pair and that from their split and vibrationally-relaxed counterparts including $1B_u^+(0)$ and $1B_u^-(0)$ or $3A_g^-(0)$, (ii) transient absorption from the $1B_u^-(0)$ state generated by internal conversion, (iii) transient absorptions from the $2A_g^-(0)$ and the T_1 state generated by internal conversion and singlet-to-triplet fission, respectively (see the set of SADS in Fig. 6).

The decay of each component, shown below in time profiles, is extremely fast, indicating singlet energy-transfer reactions through the three channels. The light-harvesting function of *not only* the $1B_u^-$ state *but also* the $3A_g^-$ state would be evidenced, when the energy-transfer efficiencies had been determined including the excited-state dynamics of BChl *a* as the accepter. Obviously, coherent excitation of the diabatic pair, i.e., $1B_u^+ + 1B_u^-$ or $1B_u^+ + 3A_g^-$, to generate quantum beat should be another powerful mechanism of enhancing the Car-to-BChl singlet-energy transfer, taking advantage of both the $1B_u^-$ and $3A_g^-$ optically-forbidden states.

REFERENCES

Christina R, Miki T, Kakitani Y, Aoyagi S, Koyama Y, Limantara L (2009) Energies and excited-state dynamics of $1B_u^+$, $1B_u^-$ and $3A_g^-$ states of carotenoids bound to LH2 antenna complexes from purple photosynthetic bacteria. *Chem Phys Lett* **480**: 289–295.

Furuichi K, Sashima T, Koyama Y (2002) The first detection of the $3A_g^-$ state in carotenoids using resonance-Raman excitation profiles. *Chem Phys Lett* **356**: 547–555.

Kakitani Y, Miki T, Koyama Y, Nagae H, Nakamura R, Kanematsu Y (2009) Vibrational relaxation and internal conversion in the overlapped optically-allowed $1B_u^+$ and optically-forbidden $1B_u^-$ or $3A_g^-$ vibronic levels of carotenoids: Effects of diabatic mixing as determined by Kerr-gate fluorescence spectroscopy. *Chem Phys Lett* **477**: 194–201.

Li C, Miki T, Kakitani Y, Koyama Y, Nagae H (2007) Negligible shift of $3A_g^-$ potential in longer-chain carotenoids as revealed by a single persistent peak of $3A_g^- \rightarrow 1A_g^-$ stimulated emission followed by $3A_g^- \leftarrow 1A_g^-$ transient-absorption. *Chem Phys Lett* **450**: 112–118.

Miki T, Kakitani Y, Koyama Y, Nagae H (2008) Stimulated emission from the $1B_u^-(0)$ level and the $1B_u^+(0) + 1B_u^-(1$ and $2)$ diabatic levels upon excitation to the $1B_u^+(0)$ level in neurosporene and spheroidene. *Chem Phys Lett* **457**: 222–226.

Sutresno A, Kakitani Y, Zuo P, Li C, Koyama Y, Nagae H (2007) Presence and absence of electronic mixing in shorter-chain and longer-chain carotenoids: Assignment of the symmetries of $1B_u^-$ and $3A_g^-$ states located just below the $1B_u^+$ state. *Chem Phys Lett* **447**: 127–133.

Tavan P, Schulten K (1986) The low-lying electronic excitations in long polyenes: A PPP-MRD-CI study. *J Chem Phys* **85**: 6602–6609.

Tavan P, Schulten K (1987) Electronic excitations in finite and infinite polyenes. *Phys Rev B* **36**: 4337–4358.

Zuo P, Sutresno A, Li C, Koyama Y, Nagae H (2007) Vibrational relaxation on the mixed vibronic levels of the $1B_u^+$ and $1B_u^-$ states in all-*trans*-neurosporene as revealed by subpicosecond time-resolved, stimulated emission and transient absorption spectroscopy. *Chem Phys Lett* **440**: 360–366.